

On-Wafer Measurements of Noise Temperature

J. Randa, Robert L. Billinger, and John L. Rice

Abstract—The NIST Noise Project has developed the theoretical formalism and experimental methods for performing accurate noise-temperature measurements on a wafer. This report summarizes the theoretical formulation and describes the design, methods, and results of tests performed to verify our ability to measure on-wafer noise temperature. Several different configurations with known off-wafer noise sources were used to obtain different, known, on-wafer noise temperatures. These were then measured, and the results were compared to predictions. Good agreement was found, with a worst-case disagreement of 2.6%. An uncertainty analysis of the measurements resulted in an estimated standard uncertainty (1σ) of 1.1% or less for most values of noise temperature. The tests also confirm our ability to produce known noise temperatures on a wafer, with an uncertainty of about 1%.

Index Terms—Noise, noise measurement, noise temperature, on-wafer noise, thermal noise.

I. INTRODUCTION

A GOOD deal of work has been done over the past several years to develop and improve techniques for measurement of noise figure on wafer [1]–[11]. There are methods and even commercial systems for such measurements. There is always room for improvement and extension of such methods, of course, but the more pressing need appears to be in the areas of accuracy assessment, traceability, and general quality assurance. To address these needs, the National Institute of Standards and Technology (NIST) is developing the capability to accurately measure thermal noise on wafer and to assess the uncertainties in such measurements [12]. This work builds on our long-established ability in noise-temperature measurements in waveguide and coaxial structures [13], [14] as well as on recent work on coaxial measurements of low-noise amplifiers [15]. A necessary first step in the development of an on-wafer noise capability is to establish the ability to measure noise temperature on wafer and to determine the accuracy of those measurements.

This paper reports the results of a series of measurements designed to test our ability to measure noise temperature on a wafer and to estimate the uncertainty in such measurements. The experiment consists of producing and then measuring a number of known on-wafer noise temperatures and comparing the measured and known values. Several different ambient-

temperature sources were used, but these do not provide a very demanding test. To produce a known (nonambient) noise temperature on a wafer, we connected a known coaxial noise source to one probe of a probe station and contacted the probe to a transmission line on the wafer. By measuring and correcting for the probe properties, we can compute the noise temperature at a reference plane in the on-wafer transmission line. We then used the second probe to measure the noise temperature at this reference plane and compared computed and measured results. Both hot and cold coaxial sources were used, enabling us to produce and measure on-wafer noise temperatures ranging from about 160 K to about 7600 K. The measurements were performed at frequencies from 7.8 GHz to 8.2 GHz.

In the next section we present the theoretical background and a summary of the equations used. Section III describes the experiment and presents the results. Section IV contains the uncertainty analysis, and in Section V we discuss the results and summarize the work.

II. THEORETICAL BACKGROUND

A. General Equations

The on-wafer environment introduces several complications to noise-temperature measurements not present in coaxial or waveguide systems. For the theoretical framework, the principal complication is the fact that on-wafer transmission lines typically have significant losses, due mostly to dielectric losses in the substrate but also to resistive losses in the thin conductor strips. The presence of these losses changes the form of the various power equations (and consequently of the mismatch factors and available-power ratios) used in computing the noise temperature of a device under test from the measured powers. Therefore, the detailed form of the radiometer equation must be reexamined and rederived. This was done in [12], and we shall just summarize the results here.

The derivation of the radiometer equation and its general form in terms of noise temperatures, powers, and ratios of powers are much the same as in the lossless case. The basic measurement configuration for a noise temperature measurement on wafer is outlined in Fig. 1, with relevant reference planes labeled. The radiometer itself also contained an isolator, so that there were isolators immediately to the left and right of plane 0. Available powers will be denoted by a capital P , and delivered powers by lowercase p . The subscript on an available power generally indicates the device, except in the case of P_a , where it indicates the ambient, $P_a = kBT_a$. The subscripts on the delivered powers and mismatch factors will

Manuscript received October 22, 1997; revised September 21, 1999. This work was supported in part by the NIST/Industrial MMIC Consortium.

The authors are with the Radiofrequency Technology Division, National Institute of Standards and Technology (NIST), Boulder, CO 80303 USA (e-mail: randa@boulder.nist.gov).

Publisher Item Identifier S 0018-9456(99)09693-X.

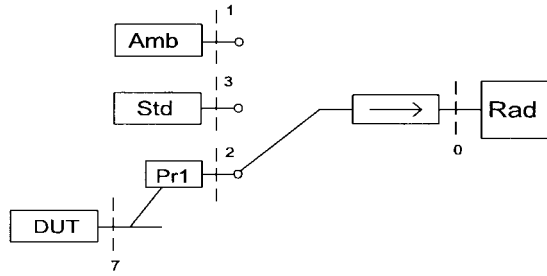


Fig. 1. Basic setup for measurement of on-wafer noise source.

indicate the reference plane and the configuration. The device under test (DUT) will be labeled by x . Thus $p_{2,x}$ refers to the delivered power at plane 2 when the DUT is connected. The power delivered to the radiometer, at plane 0, when the switch is connected to the DUT at plane 7, is given by

$$p_{0,x} = M_{0,x}\alpha_{07}P_x + M_{0,x}[1 - \alpha_{07}]P_a + p_{ex}, \quad (1)$$

where p_{ex} is the intrinsic effective input noise power of the radiometer for this configuration, α is the available power ratio, $\alpha_{07} = P_0/P_7$, and M is the mismatch factor, $M_{0,x} = p_0/P_0(x)$. Similar equations can be written for the cases when the switch is connected to the cryogenic standard at plane 3 and to the ambient standard at plane 1. Assuming perfect isolators, the three equations can be combined to yield the radiometer equation,

$$T_x = T_a + (T_s - T_a) \frac{M_{0,s}\alpha_{03} Y_x - 1}{M_{0,x}\alpha_{07} Y_s - 1} \quad (2)$$

where $Y_x \equiv p_x/p_a$ and $Y_s \equiv p_s/p_a$.

Equation (2) is a usual form for the radiometer equation for an isolated total-power radiometer. The on-wafer complications arise in the expressions for the mismatch factors and available power ratios, due to the form of the power equation for transmission lines with loss. For a transmission line with appreciable loss, assuming the presence of a single mode a , the power passing a reference plane can be written as [16], [17]

$$p_a = [|a_a|^2 - |b_a|^2 + 2 \tan \zeta_a \operatorname{Im}(a_a b_a^*)] \quad (3)$$

where a_a and b_a are the travelling-wave amplitudes in the positive and negative z directions at the plane of interest, and a particular normalization has been chosen. The phase ζ_a is a property of the mode a . If the mode has a well-defined impedance, ζ_a is the phase of that impedance. In general, it can

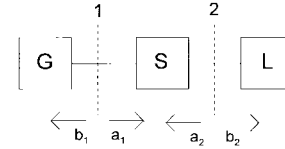


Fig. 2. Two-port between generator and load. Subscripts refer to reference plane.

be defined in terms of the modal fields [12], [17]. A method for measuring ζ in on-wafer applications has been developed by Marks and Williams [18], and we shall use that method in this work.

The presence in the power equation of the extra term, proportional to $\tan \zeta_a$, induces corresponding changes in the familiar expressions for mismatch factors and ratios of available powers, which enter into the radiometer equation. The mismatch factor at a reference plane between a source G and a load L takes the form shown in (4) at the bottom of the page, where the subscript denoting the mode has been dropped since we assume a single mode at all reference planes considered in this work. Referring to Fig. 2 for notation, we can write the available power ratio between planes i and j as

$$\alpha_{ji} \equiv \frac{P_j}{P_i} = \frac{|S_{21}|^2 [1 - |\Gamma_G|^2 - 2 \operatorname{Im} \Gamma_G \tan \zeta_i] \cos^2 \zeta_i}{|1 - \Gamma_G S_{11}|^2 [1 - |\Gamma_{GS}|^2 - 2 \operatorname{Im} \Gamma_{GS} \tan \zeta_j] \cos^2 \zeta_j} \quad (5)$$

where ζ_i and ζ_j are the phases of the modal impedances at planes i and j , and Γ_{GS} is the reflection coefficient at plane j from the source and two-port to the left of that plane,

$$\Gamma_{GS} = S_{22} + \frac{S_{12} S_{21} \Gamma_G}{1 - \Gamma_G S_{11}}. \quad (6)$$

By using (4) and (5) and a some algebra [12], we can obtain the expression for the ratio of M 's and α 's appearing in the radiometer equation

$$\frac{M_{0,s}\alpha_{03}}{M_{0,x}\alpha_{07}} = \frac{|S_{21}(3-0)|^2 [1 - \Gamma_x \Gamma_{7,r}]^2}{|S_{21}(7-0)|^2 [1 - \Gamma_s \Gamma_{3,r}]^2} \times \frac{(1 - |\Gamma_s|^2)}{\cos^2 \zeta_7 [1 - |\Gamma_x|^2 - 2 \tan \zeta_7 \operatorname{Im} \Gamma_x]} \quad (7)$$

where we have used the fact that $\zeta_3 \approx 0$, since plane 3 is in a coaxial line with real impedance, and that $S_{22}(7-0) \approx$

$$M \equiv \frac{p^{\text{del}}}{P_{\text{avail}}} = \frac{[1 - |\Gamma_L|^2 - 2 \tan \zeta \operatorname{Im} \Gamma_L][1 - |\Gamma_G|^2 - 2 \tan \zeta \operatorname{Im} \Gamma_G] \cos^2 \zeta}{|1 - \Gamma_L \Gamma_G|^2} \quad (4)$$

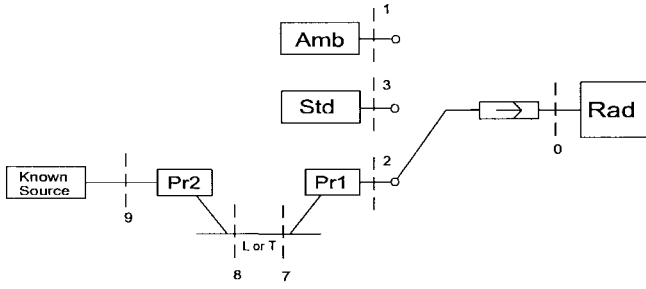


Fig. 3. Basic setup for measurements of known on-wafer noise temperatures from off-wafer standards. The L or T between planes 8 and 7 refers to the on-wafer line or through.

$S_{22}(3-0)$, due to the isolators. Equation (7) differs from the traditional (lossless) form by the presence of the $\cos^2 \zeta$ and $\tan \zeta$ terms. For the (known) sources in our tests, $\tan \zeta \approx -0.08$, and $|\text{Im} \Gamma_x|$ ranges up to about 0.15. Use of the lossless form of (7) would thus lead to errors ranging up to about 3% in our measurements.

Equations (2) and (7) can be used to determine the measured noise temperature on wafer, at plane 7. In our on-wafer tests, we also need to compute the noise temperature at plane 7 from a known noise temperature at plane 9 for the configuration of Fig. 3. This is easily done by using

$$T_7 = \alpha_{79} T_9 + [1 - \alpha_{79}] T_a \quad (8)$$

with

$$\alpha_{79} = \frac{|S_{21}(9-7)|^2 (1 - |\Gamma_s|^2)}{\cos^2 \zeta_7 [1 - \Gamma_s S_{11}(9-7)]^2 [1 - |\Gamma_{7,s}|^2 - 2 \tan \zeta_7 \text{Im} \Gamma_{7,s}]}. \quad (9)$$

In this equation, the subscript s represents whatever source is connected at plane 9.

B. Use of Pseudo-Waves

The significant losses in typical on-wafer transmission lines mean that in general it is *not* a good approximation to take the characteristic impedance to be real. Therefore, the phase ζ is nonzero, and we should use the full, cumbersome, general forms for the mismatch factors, available power ratios, etc., as derived in the preceding subsection. Simplification is possible, however. Marks and Williams [17] have suggested and developed the use of what they call “pseudo-waves,” which are linear combinations of the travelling waves, where the linear combination depends on the characteristic impedance and on a reference impedance of the user’s choice. This transformation then induces a corresponding transformation of reflection coefficients and S -parameters at the reference plane(s) affected. The advantage of pseudo-waves is that if we choose a real reference impedance (typically 50 Ω), use of pseudo-waves and their associated reflection coefficients and S -parameters results in the familiar, lossless-line form for power, $|a^2|(1 - |\Gamma|^2)$. Consequently, ratios of powers, such as mismatch factors and available power ratios, also revert to their lossless-line forms. The equations derived above for travelling

waves also hold for pseudo-waves [12], provided that the ζ ’s are taken to be the phases of the reference impedances, and provided that all reflection coefficients and S -parameters are those appropriate to the reference impedance(s) chosen.

The price that one pays for the simplifications engendered by pseudo-waves is that the reflection coefficients and S -parameters must also be transformed to the reference impedance chosen. We used the NIST-developed package MultiCal [19], with a multiline TRL calibration [20] to characterize the probes. One of the features of MultiCal is that it allows one to measure pseudo-wave quantities, and consequently we choose a reference impedance of 50 Ω and use the simplified ($\zeta = 0$) version of the equations. (MultiCal also provides for measurement of ζ , the phase of the characteristic impedance [18].) The form of the radiometer equation, (2), is unchanged, but (7) for the ratio of mismatch factors and available power ratios becomes

$$\frac{M_{0,s} \alpha_{03}}{M_{0,x} \alpha_{07}} = \frac{|S_{21}^{(50)}(3-0)|^2 |1 - \Gamma_{7,x}^{(50)} \Gamma_{7,r}^{(50)}|^2 (1 - |\Gamma_{3,s}^{(50)}|^2)}{|S_{21}^{(50)}(7-0)|^2 |1 - \Gamma_{3,s}^{(50)} \Gamma_{3,r}^{(50)}|^2 (1 - |\Gamma_{7,x}^{(50)}|^2)} \quad (10)$$

where the superscript “(50)” indicates that the reflection coefficient or S -parameter is with respect to a 50 Ω reference impedance. In computing the on-wafer noise temperature due to an off-wafer source, (8) remains the same, but (9), for the available power ratio, takes the form

$$\alpha_{79} = \frac{|S_{21}^{(50)}(9-7)|^2 (1 - |\Gamma_{9,s}^{(50)}|^2)}{|1 - \Gamma_{9,s}^{(50)} S_{11}^{(50)}(9-7)|^2 [1 - |\Gamma_{7,s}^{(50)}|^2]}. \quad (11)$$

If our on-wafer methods and software had measured only travelling-wave quantities, then it could be more convenient to use (7) as derived, with the measured travelling-wave reflection coefficients and S -parameters and the measured ζ .

III. EXPERIMENTAL SETUP AND RESULTS

A. Experimental Setup

Fig. 1 contains a simple block diagram of the general experimental setup for a one-port device on a wafer, with relevant reference planes numbered. The radiometer was switched between the ambient standard noise source (plane 1), the nonambient standard noise source (plane 3), and the on-wafer DUT (plane 7), measuring and recording the delivered power from each. The nonambient standard was usually the NIST cryogenic coaxial (GPC-7) primary standard [21], which was connected at plane 3. For some of the measurements, a previously calibrated, high-temperature check standard was used as the nonambient standard. This was done when the cryogenic standard was being used elsewhere in the measurement or when we measured an on-wafer noise diode of very high noise temperature.

Detail of the detection system is shown in Fig. 4. The rf frequencies that contribute to the output power are in the range $f = f(LO) \pm 5$ MHz. The detection unit was designed and constructed to be *very* stable. Tests indicate that its output is stable within ± 0.001 dB/12 h. The other critical feature

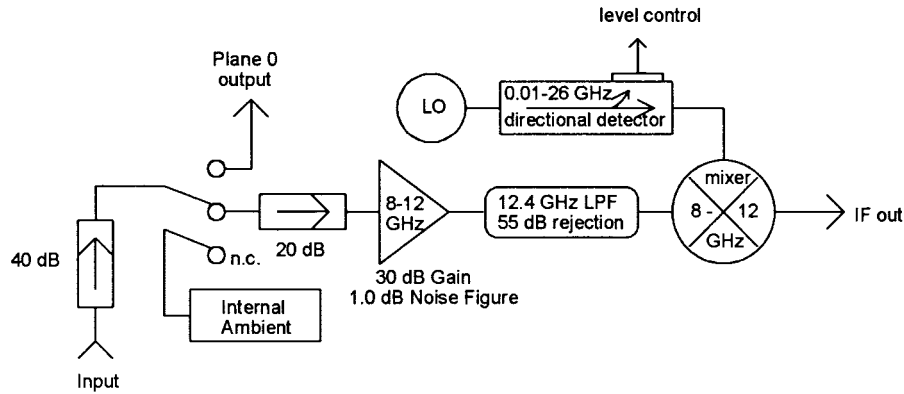


Fig. 4. Detail of radiometer.

of the detection unit is its linearity. The IF subsystem is the potential problem since it must handle the greatest power. The IF subsystem was tested and found to be linear within ± 0.005 dB for every 3 dB of detected power up to 17 mW. Our typical measurements were done at IF powers less than 2 mW, and all measurements were kept well within the linear range.

The detection unit was held at a fixed temperature by mounting it on a brass plate, through which ambient-temperature water was circulated. Water was also circulated through the switch assembly, the IF system, and the ambient standard. The temperature of the ambient standard was measured continuously with a calibrated thermistor. "Ambient" temperature is used to mean the temperature of the ambient standard, typically about 296.0 K. Room temperature could differ from the "ambient" by as much as 2 K. The temperature of the circulating water was within 0.1 K of ambient.

The probe station was modified so that probe 1 remained fixed during the entire experiment. This was done to minimize the risk of changes in reflection coefficients and S -parameters to the right of plane 7. The wafer was positioned by moving the chuck, which was controlled by a jig built for that purpose. For most of the noise sources we measured, there was little worry about on-wafer heating. The one case in which it was a concern was for the on-wafer noise diode. In that case, we divided the (multiple-measurement) run into halves and into thirds and checked for noise temperature change as a function of time. No significant difference was found, indicating that if the physical temperature of the diode was rising, it was not affecting the noise temperature.

To obtain known on-wafer noise temperatures, the configuration of Fig. 3 was used, with known off-wafer noise sources attached at plane 9. In some cases the known source was connected directly to the probe at plane 9. In other cases a flexible cable was used; the cable-probe connection was then plane 9, and the source-cable connection was called plane 10. When a cable was used, it was held securely in place throughout the measurements, to minimize changes in the measured S -parameters.

We used the radiometer equation, (2), to compute the noise temperature T_x of the DUT from the delivered powers measured by the radiometer. Equation (10) was used for the

ratio of mismatch factors and available-power ratios, requiring the measurement of the various reflection coefficients and S -parameters. The S -parameters and reflection coefficients to be measured included $S_{21}(3-0)$, $S_{21}(7-0)$, Γ_x , $\Gamma_{7,r}$, Γ_S , and $\Gamma_{3,r}$. The two subscripts on some of the reflection coefficients refer to the reference plane and the direction, with r referring to the radiometer direction. S -parameters [$S_{ij}(2-0)$, $S_{ij}(3-0)$] from the switch ports through the switch to plane 0, between the two isolators, were measured with a vector network analyzer (VNA). When the reference plane occurred at a connector (planes 2, 3, 9, 10), it was taken at the center of the connector, which was GPC-7 in all such cases. The radiometer has a port which allows access to plane 0. The reflection coefficients (Γ_S) of the cryogenic standard and the high-temperature check standard were also measured with the VNA. For $\Gamma_{3,r}$ we used $\Gamma_{3,r} \approx S_{11}(3-0)$. The accuracy of this approximation can be inferred from a comparison of $\Gamma_{7,r}$, which was measured, to $S_{11}(7-0)$, which can be constructed from the measured $S(7-2)$ and $S(2-0)$. This comparison indicated that the approximation was accurate within 0.07 in the real and imaginary parts of $\Gamma_{3,r}$ (0.1 in the magnitude).

On-wafer quantities were measured using MultiCal [19]. An on-wafer multiline TRL calibration [20] was performed. The calibration kit consisted of a through, a reflect, and three transmission lines of different lengths, all of gold on a GaAs wafer. It was fabricated by the NIST High-Speed Microelectronics Project. In the calibration, the probes were defined to extend to the center of the through in the TRL calibration standards. The through is 0.50 mm long, and thus plane 7 is 0.25 mm from the probe-1 end of the through. Each probe thus includes a short (0.25 mm) section of coplanar waveguide (CPW), of which about 0.225 mm is between the probe tip and the reference plane, and 0.025 mm is behind the probe tip. In principle this length is chosen long enough to assure a single mode at planes 7 and 8. The on-wafer calibration provides a measurement of $S_{ij}(7-2)$ and $S_{ij}(9-8)$. It also extends the VNA calibration to the reference planes 7 and 8 on wafer. The VNA and MultiCal can then be used to measure reflection coefficients at plane 7, both of the radiometer ($\Gamma_{7,r}$) and of the DUT (Γ_x). A number of different on-wafer DUT's were measured (discussed below), and for

each the reflection coefficient was measured at plane 7. The S -parameters $S_{ij}(7-0)$ between planes 0 and 7 were not measured directly but were obtained by cascading $S_{ij}(7-2)$ and $S_{ij}(2-0)$.

In the course of the VNA and MultiCal measurements, a good deal of redundant information was obtained. We used this information to perform checks on our methods and measurements. For example, $\Gamma_{7,r}$, $\Gamma_{2,r}$, and $S(7-2)$ were all measured separately, but $\Gamma_{7,r}$ must equal the result of cascading $S(7-2)$ and $\Gamma_{2,r}$. A number of such checks were performed, and agreement was typically within a few percent. The probes were calibrated before and after the on-wafer measurements, and the largest difference in S_{21} for either probe was 0.17%. The averages of several VNA measurements for the reflection coefficients of the primary standard and check standard were compared to results of independent measurements by personnel of the NIST Six-Port Project at 8.0 GHz. The two agreed within ± 0.001 . A number of other repeatability checks were performed, with similar results. These checks give us confidence that we are correctly measuring the reflection coefficients and S -parameters.

B. Noise Sources Measured

The purpose of the experiment was to test our ability to measure noise temperature on a wafer and to estimate the uncertainties in such measurements. In addition, we wanted to resolve two specific questions which had arisen in preliminary measurements. One was whether any (nonambient) radiation was entering the system through the open, on-wafer transmission line, thereby adding additional power to the lines and corrupting the noise measurements. The other issue was whether flexible cables could be used to connect off-wafer sources to one of the probes and thus to a transmission line on the wafer. Earlier tests had suggested that the cables could introduce variations as large as about 12% in the noise-temperature measurement, which was considerably larger than we were willing to tolerate.

To address these questions, we measured a number of different noise sources. We began with an off-wafer measurement of a high-temperature check standard with a known noise temperature. This provided a check that the new radiometer and the associated computations were functioning properly. The first on-wafer noise source was just a resistor on a GaAs wafer. The leads from the resistor were the same as the CPW line used in the on-wafer calibration kit. Reference plane 7, at which we measured the noise temperature, was therefore a distance 0.25 mm from the end of the CPW (about 0.225 mm from the tip of the probe), as discussed near the end of Section III-A. Since the resistor was at the same (room) temperature as the line, the exact location of the reference plane was not especially important in this measurement, but in other measurements it is critical. The resistor was in equilibrium with its surroundings, at room temperature. As discussed above, room temperature may not have been exactly “ambient” temperature, but it was close (within about 2 K). Measurement of the resistor’s noise temperature constitutes a (not very demanding) test of the measurement methods and

system. It also provides a test of whether outside radiation was entering the system. If the resistor and transmission line were absorbing (nonambient) radiation from the surrounding environment, then the measured noise temperature would differ from the room or ambient temperature. Preliminary experiments indicated that a nearby incandescent lamp could affect the measured noise temperature. Such obvious local sources were removed, but there were still the fluorescent room lights, emissions from equipment in the room, and various external sources—the room is shielded, but not very well.

In order to properly test our ability to measure noise temperature on a wafer, we needed nonambient, on-wafer noise sources with known noise temperatures. Such sources were not available, and so we produced known noise temperatures on wafer by using known off-wafer noise sources. The configuration is shown in Fig. 3. A check standard with known noise temperature was connected to probe 2 at plane 9, and probe 2 was then connected to an on-wafer transmission line at plane 8. The transmission line was one of those in the calibration kit mentioned in Section III-A; both the through and the longest line (6.565 mm between planes 7 and 8) of the kit were used. Since the properties of probe 2 were determined by the on-wafer calibration, and since the properties of the through and the line were known, we were able to use (8) and (11) to calculate the noise temperature at plane 7 on wafer in terms of the known noise temperature at plane 9. The calculated value could then be compared to the measurement result. We also connected an ambient source at plane 9, with both the line and the through on wafer, and measured the resulting noise temperatures at plane 7. The cryogenic primary standard must remain vertical, and therefore it could not be connected directly to plane 9. It was connected by a flexible cable, with the connection between the cable and standard labeled as plane 10. The check standard was also attached at plane 10. For both cases both the through and the line were used on the wafer, and the noise temperature at plane 7 was calculated and measured in each case. In measurements with the cable, great care was taken to minimize any movement or flexing of the cable between the time its properties were measured on the VNA and the time of the measurement of the noise temperatures.

The final source was a noise diode bonded to a short section of CPW line on a GaAs wafer, with no attenuating circuit to control the reflection coefficient. The on-wafer configuration is shown in Fig. 5. Bias for the diode was supplied through probe 1 from a monitored current source. The section of CPW to the left of plane 7 is the same as that used in the calibration kit, and therefore the on-wafer calibration and characterization of probe 1 was still applicable. Two problems rendered this diode source less than ideal. The lack of an attenuator meant that its reflection coefficient was not very well matched to the line or probe and that it could exhibit rather erratic behavior as a function of frequency. In addition, there was no independent method of determining the noise temperature of the diode. We therefore have no way of checking that the answer we obtained is correct. Nevertheless, the exercise provided experience in measuring an unknown source with very high noise temperature. Because the diode is not a linear

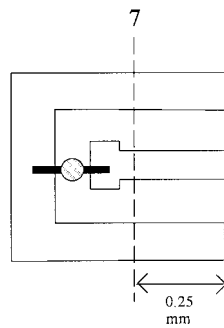


Fig. 5. On-wafer noise diode (shaded circle) bonded to coplanar waveguide.

device, its reflection coefficient may depend on the incident power. In measuring its noise temperature, we are interested in its reflection coefficient (Γ_D) for very low power. We measured Γ_D for three different values of incident power, including the lowest allowed by our VNA. The power levels from the synthesizer of the VNA were -9 dB, -10 dB, and -11 dB, all relative to 1 mW. The corresponding powers incident on the diode were roughly 11 dB lower. We found that Γ_D varied little over the range measured, and was unchanged within measurement accuracy between the two lowest powers. Consequently, the value at the lowest power should be valid for the incident powers encountered in the noise temperature measurement.

To facilitate discussion of the different measurement configurations, we introduce some additional notation. Each configuration will be labeled by the plane at which the noise temperature was measured and what was connected at that plane. We will use Cr to denote the cryogenic primary standard, Ck for the check standard, A for an ambient load, R for the on-wafer resistor, D for the on-wafer noise diode, L for the on-wafer calibration-kit line, T for the on-wafer calibration-kit through, and the respective number for each reference plane. Thus the measurements of the on-wafer diode and resistor are 7D and 7R respectively; the ambient load connected at plane 9 with the line on wafer is 7L9A; the cryogenic primary standard connected through the cable with the through on wafer is 7T10Cr; etc.

To summarize, we measured a variety of noise sources, providing a range of significant tests of our ability to measure noise temperature on wafer. The direct measurement of the check standard tested the off-wafer aspects of the system, including the radiometer, the switch assembly, and a portion of the data-analysis software. The on-wafer noise diode measurement (7D) allowed us to measure an unknown noise source with very high noise temperature (nearly 10^6 K). It tested whether we could get an answer for such a device, but we do not know what the correct answer is. The three measurements of ambient loads (7R, 7T9A, and 7L9A) provided a test of our ability to measure a known noise temperature, albeit a rather easy one since measurement of an ambient load is insensitive to some common errors. Since the ambient measurements involved three different on-wafer configurations, they did provide a very good test of whether any (nonambient) outside radiation was getting into the system.

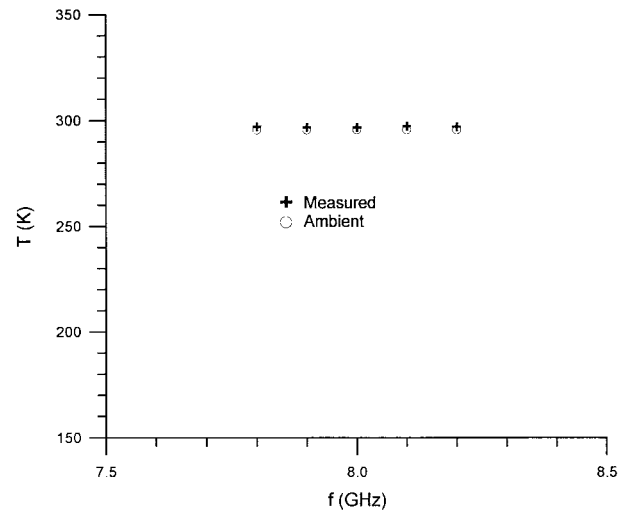


Fig. 6. On-wafer noise temperature for configuration using on-wafer room-temperature resistor (7R).

The remaining six noise-temperature measurements were a good test of our entire system and methods. The two using the cryogenic primary standard (7T10Cr, 7L10Cr) tested our ability to measure low noise temperatures (about 160 K and 180 K) on wafer, and the four using the check standard (7T9Ck, 7L9Ck, 7T10Ck, 7L10Ck) tested our ability to measure high temperatures (about 5000 K to 7600 K). The fact that we measured the check standard both when it was connected directly to probe 2 at plane 9 and when it was connected to the cable at plane 10 enabled us to identify problems introduced by the flexible cable.

C. Results

Measurements were made from 7.8 GHz to 8.2 GHz in increments of 0.1 GHz. The frequencies were chosen in order to compare to earlier, preliminary measurements. The frequency range will be expanded in future tests. The first test performed was the direct (off-wafer) measurement of the noise temperature of the check standard. The results were compared to results of previous measurements of the same device using the present system and to an earlier measurement using the traditional NIST radiometer. The agreement was excellent. The present result at 8.0 GHz differs from the result on the older system by 4 K, out of 9238 K (0.04%). The two sets of measurements on the present system differed by at most 0.15%. We concluded that the radiometer was functioning properly for off-wafer measurements and that its repeatability is very good.

Rather than present all the on-wafer results in detail, we shall show some representative results and summarize the agreement between measured and predicted values. Full results are contained in [12]. Three room-temperature loads were measured: the on-wafer resistor (7R), and the off-wafer room-temperature load measured through both an on-wafer through (7T9A) and a line (7L9A). In all three cases, the agreement between the measured noise temperature and the ambient temperature was very good. The on-wafer resistor results are

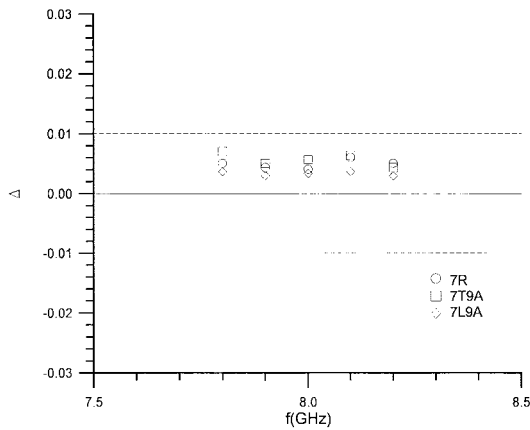


Fig. 7. Fractional differences between measured and predicted on-wafer noise temperatures for room-temperature sources.

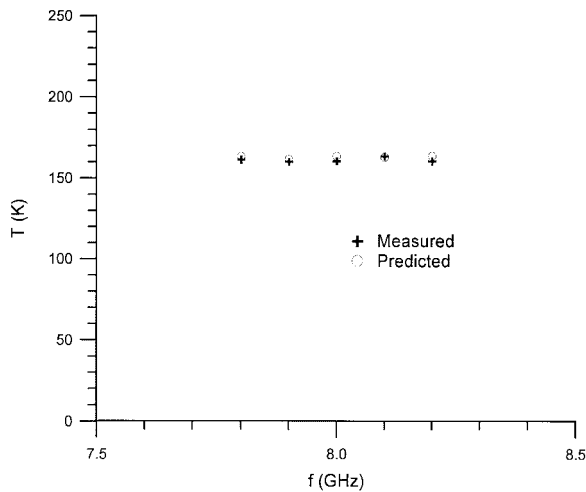


Fig. 8. On-wafer noise temperature for configuration using cryogenic source, cable, on-wafer through (7T10Cr).

typical; they are shown in Fig. 6. The fractional difference between measured and ambient temperatures

$$\Delta \equiv 2 \frac{T(\text{measured}) - T(\text{predicted})}{T(\text{measured}) + T(\text{predicted})} \quad (12)$$

is plotted in Fig. 7, where the predicted noise temperature is the ambient temperature in this case. The measured noise temperature is consistently about 0.5% (1.5 K) above the ambient temperature. As discussed in Section III-A, even this small discrepancy can be attributed to the fact that the sources being measured were at “room” rather than “ambient” temperature, and the two can differ by as much as 2 K. We therefore conclude that our system and methods correctly measure on-wafer noise temperatures near ambient. Because the three ambient loads measured corresponded to three different configurations on wafer (resistor, through, line), the fact that none of the three exhibited signs of external radiation effects is a strong indication that such effects are absent in our on-wafer noise measurements.

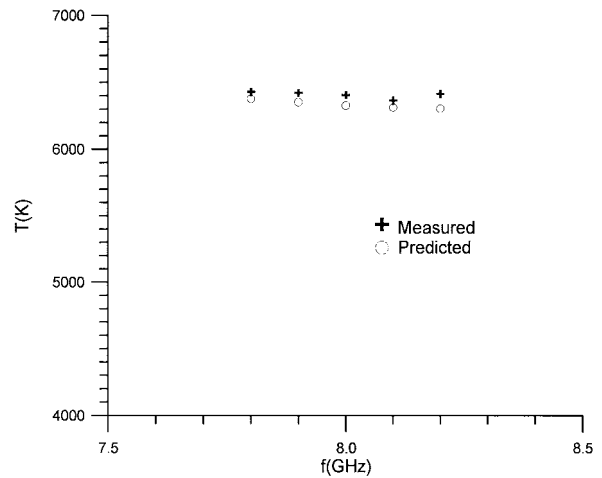


Fig. 9. On-wafer noise temperature for configuration using high-temperature source, on-wafer line (7L9Ck).

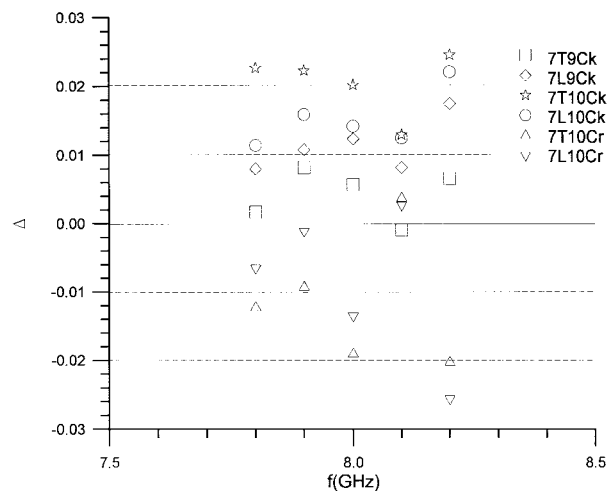


Fig. 10. Fractional differences between measured and predicted on-wafer noise temperatures for nonambient sources.

Fig. 8 shows the results for the cryogenic standard connected through a cable to the probe, with the through on wafer (7T10Cr), and Fig. 9 presents the results for the check standard connected directly to the probe, with the line on wafer (7L9Ck). The predicted results are the noise temperatures at plane 7 calculated from the known noise temperatures of the cryogenic or check standard and the measured properties of probe 2 with the cable or line, as appropriate. Agreement between measured and predicted noise temperatures in the figures is good, and it is representative of the other nonambient configurations as well. The comparison of measurement and prediction for nonambient, on-wafer noise temperatures is summarized in Fig. 10, which plots the Δ of (12) for each of the six known nonambient temperatures we measured. Most of the points lie in the $|\Delta| \leq 2\%$ range, with a few between 2.0% and 2.6%.

Finally, in Fig. 11, we show the noise temperature measured for the on-wafer noise diode. As we discussed above, we do not know the diode’s noise temperature from other informa-

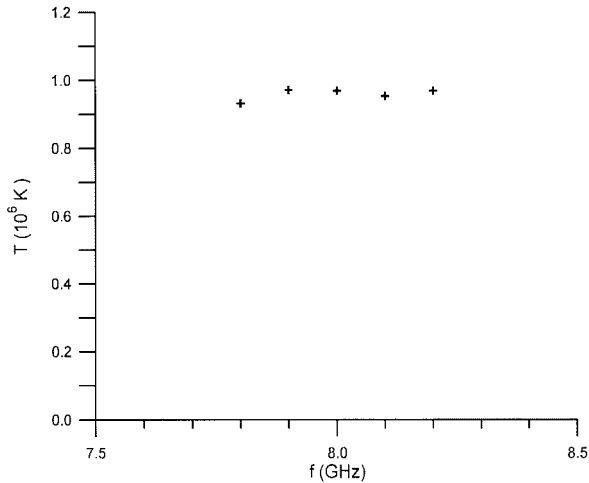


Fig. 11. Measured noise temperature of on-wafer diode (7D).

tion. The measurement indicates that the noise temperature of the diode is very high, approaching 10^6 K. In order not to saturate the radiometer, an attenuator was introduced in front of it, between plane 2 and the first isolator. This in turn lowered the power from the cryogenic standard unacceptably, and so the previously measured high-temperature check standard was used as the nonambient standard in this measurement.

IV. UNCERTAINTY ANALYSIS

To assess the significance of the differences between measurement and prediction in the preceding section, we need to estimate the uncertainties in both the measured and the predicted values. We must also consider the correlation between possible errors in measurement and prediction. The comparison we performed magnifies some potential errors and is insensitive to others. We will first present an uncertainty analysis for our measurements of noise temperature on wafer. We will then consider uncertainties in the predictions and in the Δ defined by (12).

The noise temperature of the DUT is calculated from the radiometer equation, (2). This form assumes a perfect isolator as well as a linear radiometer. Uncertainties in T_x arise due to uncertainties in the determination of the quantities appearing on the right side of (2) and due to departures from perfect isolation and linearity. For the present analysis, we will be concerned with the uncertainties arising in a single measurement of T_x . In keeping with the notation of the ISO [22], [23], we will use u_{T_x} to denote the standard uncertainty in the measurement of T_x . The combined standard uncertainty is composed of type-A and type-B uncertainties. Type-A uncertainties are those that are measured and determined by statistical methods, typically the standard deviation of the mean of several independent measurements of the quantity of interest. Type-B uncertainties are those determined by other means, such as estimates of systematic uncertainties. We shall deal primarily with type-B uncertainties; type-A uncertainties arise in measurement of the powers, but enough samples were taken that these uncertainties are negligible in the present experiment. We use \mathcal{E}_z to denote the fractional

standard uncertainty in the parameter z , for example, $\mathcal{E}_{\text{Cry}} \equiv u_{T_{\text{Cry}}}/T_{\text{Cry}}$.

The uncertainty in the noise temperature of the cryogenic standard contributes to the uncertainty in T_x as

$$\frac{u_{T_x}(\text{Cry})}{T_x} = \left| 1 - \frac{T_a}{T_x} \right| \left| \frac{T_S}{T_a - T_S} \right| \mathcal{E}_{\text{Cry}}. \quad (13)$$

The fractional uncertainty in the GPC-7 cryogenic standard which was used in all the measurements (except of the on-wafer diode) is about 1% at 8 GHz. This results in an uncertainty of roughly 0.35% in T_x for T_x much larger than T_a .

The contribution of the uncertainty in the ambient standard temperature to the uncertainty in the DUT noise temperature is given by

$$\frac{u_{T_x}(\text{Amb})}{T_x} = \left| \frac{T_x - T_s}{T_a - T_s} \right| \frac{T_a}{T_x} \mathcal{E}_{T_a}. \quad (14)$$

The uncertainty in the ambient temperature is $u_{T_a} = 0.1$ K, or $\mathcal{E}_{T_a} = 0.034\%$. The type-A uncertainty in the ambient temperature measurement was evaluated in one of the tests. It was found to be 0.015 K, or 0.005%, and was therefore assumed negligible in all the measurements. The ambient-temperature contribution to u_{T_x} is negligible for most values of T_x , except near $T_x = T_a$, where the other uncertainties vanish.

The uncertainty in the power ratio measurements (Y_S and Y_x) was evaluated in [24], where it was found to be negligible. A similar analysis in the present case results in $\mathcal{E}_Y \leq 0.05\%$, which can be safely neglected. The linearity of the detection unit of the radiometer was discussed in Section III-A. The powers involved in the present measurements are less than 2.5 mW. Any error due to radiometer nonlinearity for these powers is negligible. The uncertainty due to finite (40 dB) isolation can be evaluated following the calculation in [14], with appropriate changes for 40 dB isolation rather than the 50 dB assumed there. This leads to an uncertainty in T_x of about 0.1% for small values of T_x and much less for large values of T_x . We neglect this contribution to u_{T_x} .

The final contribution to u_{T_x} is due to uncertainties in the measurement of the various S -parameters and reflection coefficients which appear in the expression for $(M_{0,S\alpha_{03}})/(M_{0,x\alpha_{07}})$, (10). If we use \mathfrak{R} to denote this ratio of $M\alpha$'s, and compute the variation in \mathfrak{R} due to small variations in the S -parameters and reflection coefficients, we obtain

$$\frac{\delta\mathfrak{R}}{\mathfrak{R}} = 2 \left(\frac{\delta|S_{21}(3-0)|}{|S_{21}(3-0)|} + \frac{\delta|S_{21}(7-0)|}{|S_{21}(7-0)|} \right) + D_\Gamma. \quad (15)$$

D_Γ is a rather lengthy expression containing variations in the reflection coefficients. The largest term in D_Γ is $2|\Gamma_x|\delta|\Gamma_x|$. In the present comparisons $|\Gamma_x|$ is typically less than 0.1, and this term can be neglected ($D_\Gamma \lesssim 0.2\%$). For less well matched conditions (such as the bare diode, where $|\Gamma_x| \sim 0.5$) D_Γ can be significant, and the uncertainty will be somewhat larger than the present estimate. Neglecting D_Γ , we obtain

$$\frac{u_{T_x}(\mathfrak{R})}{\mathfrak{R}} \approx 2 \left| 1 - \frac{T_a}{T_x} \right| \sqrt{\frac{u_{|S_{21}(3-0)|}^2}{|S_{21}(3-0)|^2} + \frac{u_{|S_{21}(7-0)|}^2}{|S_{21}(7-0)|^2}}. \quad (16)$$

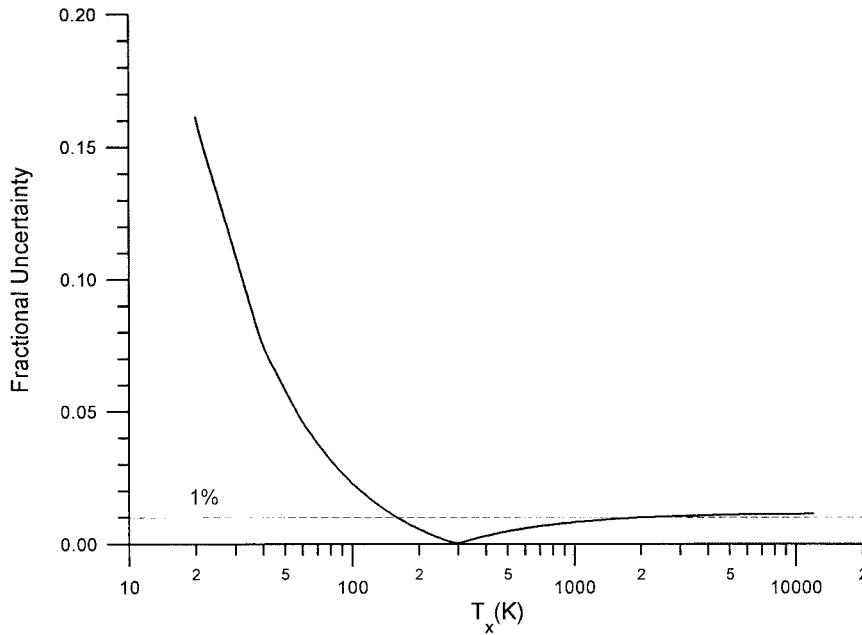


Fig. 12. Fractional uncertainty (1-sigma) in on-wafer noise-temperature measurements.

The magnitude of $S_{21}(3 - 0)$ is determined by a coaxial VNA measurement. From the manufacturer’s specifications, the fractional uncertainty in this measurement is 0.19%. The uncertainty in $S(7 - 0)$ is more complicated since it is formed by cascading $S(7 - 2)$ and $S(2 - 0)$. The fractional uncertainty in the magnitude of $S_{21}(2 - 0)$ is the same as that for $S_{21}(3 - 0)$, 0.19%. The uncertainty in the magnitude of $S_{21}(7 - 2)$ is more problematic. Repeatability of such measurements was checked both with the Verify feature of the MultiCal program and by comparing results of repeat measurements. This led to a type-A uncertainty of 0.2% in the magnitude of $S_{21}(7 - 2)$. The type-B uncertainty has two components, one due to the VNA measurements and the other due to the on-wafer calibration. Using the manufacturer’s specifications for the VNA uncertainty and typical values for $S_{21}(7 - 2)$ and $S_{21}(9 - 8)$, we obtain a fractional uncertainty in $S_{21}(7 - 2)$ due to the VNA measurements of 0.15%. The uncertainty due to the on-wafer calibration (imperfect calibration standards, etc.) is difficult to assess. We estimate that it is double the uncertainty in the VNA measurements and use $u(\text{o-w cal}) \approx 0.003$, $u(\text{o-w cal})/|S_{21}(7 - 2)| \approx 0.4\%$. Combining the various (independent) components of the uncertainty, we obtain 0.47% for the a fractional uncertainty in $|S_{21}(7 - 2)|$. The fractional uncertainty in $|S_{21}(7 - 0)|$ is then 0.51%, and (16) for the fractional uncertainty in the ratio of mismatch factors and α ’s becomes

$$\frac{u_{T_x}(\mathfrak{R})}{T_x} \approx 0.011 \times \left| 1 - \frac{T_a}{T_x} \right|. \quad (17)$$

Our estimate for the standard uncertainty in the measurement of T_x is then

$$\frac{u_{T_x}}{T_x} = \sqrt{\frac{u_{T_x}^2(\text{Cry})}{T_x^2} + \frac{u_{T_x}^2(\text{Amb})}{T_x^2} + \frac{u_{T_x}^2(\mathfrak{R})}{T_x^2}}, \quad (18)$$

with the individual components given by (13), (14), and (17). This result is plotted as a function of the DUT noise temperature in Fig. 12. For DUT noise temperatures down to about 150 K, the uncertainty is below about 1.1%. For lower temperatures, the fractional uncertainty increases, but the standard uncertainty remains below 3.5 K. For comparison, a typical standard uncertainty for our calibrations of coaxial noise sources is about 0.6% or 0.7% at this frequency. The dominant component of the uncertainty is $u_{T_x}(\mathfrak{R})$, which by itself accounts for an uncertainty of about 1% in the DUT noise temperature (for large T_x). It is unfortunate that this dominant component is also the one which is most approximate, due to our ignorance of the uncertainty in the on-wafer calibration. Our uncertainty estimate is therefore tentative at this time, although we do have evidence that it is not grossly wrong, as discussed below.

In comparing measured to predicted on-wafer noise temperatures, we also must take into account the uncertainty in the predictions. The predicted noise temperature is calculated from (8), where plane 9 is replaced by plane 10 when the cable is used. The two principal sources of uncertainty are in T_9 , the noise temperature of the known source which is connected at plane 9 (or 10), and in α_{79} , the available power ratio between planes 7 and 9 (or 10). A treatment similar to that above [12] leads to a fractional uncertainty in the calculated value of T_7 of about 0.8% for the low values of T_7 and about 1.1% for large T_7 .

These numbers are not directly applicable to the difference between measurement and prediction, however, because the uncertainties in measured and predicted noise temperatures are highly correlated. The correlations were treated in [12], where it was estimated that the uncertainty in Δ can be as large as about 1.7% for low noise temperature and about 2% for high noise temperature. All these uncertainties correspond approx-

imately to 1σ . For a 95% level of confidence (2σ), we would double all the values. We return then to the discrepancies between measurement and theory, the Δ plotted in Fig. 10. For the high noise temperatures (7T9Ck, 7L9Ck, 7T10Ck, and 7L10Ck), $|\Delta| \leq 2.5\%$. This is consistent with the estimated uncertainties. For the low temperatures, $|\Delta| \leq 2.1\%$ except for one point, where $|\Delta| = 2.56\%$. This also is consistent with the estimated uncertainties, provided that the uncertainties in measurement and prediction are correlated. We conclude that our measurement results agree with the predictions as well as should be expected. We also regard the agreement as an indication that our estimate of the uncertainty is not grossly wrong.

V. DISCUSSION AND SUMMARY

The tests confirm both that we can measure noise temperature on a wafer and that we can produce known on-wafer noise temperatures using off-wafer sources. Measurements of ambient loads agreed with room temperature to within about 0.5%, which is less than the uncertainty in the room temperature. Any effect of outside radiation entering the system was negligible. Results for nonambient noise temperatures agreed with predictions within the estimated expanded ($k = 2$) uncertainty. The estimate of the standard uncertainty was 1.1% or less for noise temperatures above about 150 K. For lower noise temperatures, the *fractional* uncertainty increased, but the standard uncertainty remained below 3.5 K. Performing measurements through a flexible cable did not degrade the accuracy noticeably, provided that great care was taken to minimize movement of the cable during the course of the experiment. All measurements on wafer were performed using probes with appreciable loss (about 1.5 dB). Future measurements will use less lossy probes, resulting in a slight decrease in the uncertainty.

While successful, the tests did have limitations. Only a narrow band of frequencies was measured (7.8 GHz to 8.2 GHz). In addition, our comparison of measured and predicted results was insensitive to certain errors in the measurement of the S -parameters of the probes. The tests were sensitive to the product of the available-power ratios of the two probes, but not to the available-power ratio of either probe individually. These points constitute significant shortcomings of the set of tests described in this paper, shortcomings which will be remedied in future experiments.

ACKNOWLEDGMENT

The authors are grateful to D. F. Wait for valuable comments and assistance in designing the experiment, D. Williams and D. Walker for extensive help in using MultiCal for on-wafer measurements, and L. Dunleavy of the University of South Florida for comments and suggestions.

REFERENCES

[1] M. S. Gupta, O. Pitzalis, S. E. Rosenbaum, and P. T. Greiling, "Microwave noise characterization of GaAs MESFET's: Evaluation by on-wafer low-frequency output of noise current measurement," *IEEE Trans. Microwave Theory Tech.*, vol. MTT-35, pp. 1208–1218, Dec. 1987.

- [2] A. C. Davidson, B. W. Leake, and E. Strid, "Accuracy improvements in microwave noise parameter measurements," *IEEE Trans. Microwave Theory Tech.*, vol. 37, pp. 1973–1978, Dec. 1989.
- [3] V. Adamian, "2–26.5 GHz on-wafer noise and S -parameter measurements using a solid state tuner," in *34th ARFTG Conf. Dig.*, Ft. Lauderdale, FL, 1989, pp. 33–40.
- [4] L. Dunleavy, "A Ka-band on-wafer s -parameter and noise figure measurement system," in *34th ARFTG Conf. Dig.*, Ft. Lauderdale, FL, 1989, pp. 127–137.
- [5] B. Hughes and P. Tasker, "Improvements to on-wafer noise parameter measurements," in *36th ARFTG Conf. Digest*, Monterey, CA, 1990, pp. 16–25.
- [6] C. Woodin, D. Wandrei, and V. Adamian, "Accuracy improvements to on-wafer amplifier noise figure measurements," in *38th ARFTG Conf. Dig.*, San Diego, CA, 1991, pp. 129–138.
- [7] G. Dambrine, H. Happy, F. Danneville, and A. Cappy, "A new method for on wafer noise measurement," *IEEE Trans. Microwave Theory Tech.*, vol. 41, pp. 375–381, Mar. 1993.
- [8] A. Caddemi and M. Sannino, "Comparison between complete and simplified methods for determining the microwave noise parameters of HEMT's," in *43th ARFTG Conf. Dig.*, San Diego, CA, 1994, pp. 121–126.
- [9] J. R. Fenton, "Noise parameter data comparison while varying the on-wafer S -parameter calibration technique," in *44th ARFTG Conf. Dig.*, Boulder, CO, 1994, pp. 89–97.
- [10] A. Boudiaf, C. Dubon-Chevallier, and D. Pasquet, "Verification of on-wafer noise parameter measurements," *IEEE Trans. Instrum. Meas.*, vol. 44, pp. 332–335, Apr. 1995.
- [11] A. Boudiaf and A. Scavenne, "Experimental investigation of on-wafer noise parameter measurement accuracy," in *1996 IEEE MTT-S Int. Microwave Symp. Dig.*, San Francisco, CA, 1996, vol. 3, pp. 1277–1280.
- [12] J. Randa, "Noise temperature measurements on wafer," Nat. Inst. Stand. Technol. Tech. Note 1390, Mar. 1997.
- [13] C. K. S. Miller, W. C. Daywitt, and M. G. Arthur, "Noise standards, measurements, and receiver noise definitions," *Proc. IEEE*, vol. 55, pp. 865–877, June 1967.
- [14] W. C. Daywitt, "Radiometer equation and analysis of systematic errors for the NIST automated radiometers," Nat. Inst. Stand. Technol. Tech. Note 1327, Mar. 1989.
- [15] D. F. Wait and J. Randa, "Amplifier noise measurements at NIST," *IEEE Trans. Instrum. Meas.*, vol. 46, pp. 482–485, Apr. 1997.
- [16] N. Marcuvitz, *Waveguide Handbook*. New York: McGraw-Hill, 1951.
- [17] R. Marks and D. Williams, "A general waveguide circuit theory," *J. Res. Nat. Inst. Stand. Technol.*, vol. 97, pp. 533–562, Sept./Oct. 1992.
- [18] R. Marks and D. Williams, "Characteristic impedance determination using propagation constant measurement," *IEEE Microwave Guided Wave Lett.*, vol. 1, pp. 141–143, June 1991.
- [19] R. Marks and D. Williams, NIST/Industrial MMIC Consortium Software Manuals, Feb. 1992.
- [20] R. Marks, "A multiline method of network analyzer calibration," *IEEE Trans. Microwave Theory Tech.*, vol. 39, pp. 1205–1215, July 1991.
- [21] W. C. Daywitt, "A coaxial noise standard for the 1 GHz to 12.4 GHz frequency range," Nat. Bur. Stands. (U.S.) Tech. Note 1074, Mar. 1984.
- [22] ISO, *Guide to the Expression of Uncertainty in Measurement*. International Organization for Standardization, Geneva, Switzerland, 1993.
- [23] B. N. Taylor and C. E. Kuyatt, "Guidelines for evaluating and expressing the uncertainty of NIST measurement results," Nat. Inst. Stand. Technol. Tech. Note 1297, Sept. 1994.
- [24] S. P. Pucic, "The uncertainty in Y -factor measurements," in *URSI Nat. Radio Sci. Meeting Dig.*, Boulder, CO, 1995, p. 39.



J. Randa received the Ph.D. degree in physics from the University of Illinois, Urbana, in 1974.

He then successively held postdoctoral or faculty positions at Texas A&M University, College Station, the University of Manchester, Manchester, U.K., and the University of Colorado, Boulder. During this time, he did research on the phenomenology of elementary particles and on theories of fundamental interactions. In 1983, he joined what is now the RF Technology Division of the National Institute of Standards and Technology (NIST), Boulder, CO.

From 1983 until early 1994, he was in the Fields and Interference Metrology Group, where he worked on characterization of electromagnetic environments, probe development, and other topics in EMI metrology. He is now in the RF Electronics Group, working in the area of thermal noise.



Robert L. Billinger received the A.A. degree in electronics technology from Wichita Technical Institute, Wichita, KS, in 1979.

From 1979 through 1984, he was with PureCycle Corporation, where he became Manager of Electronic Production and Test. Since 1985, he has been with the Radiofrequency Technology Division, National Institute of Standards and Technology (NIST), Boulder, CO, in the Radiofrequency Electronics Group. He works in the area of thermal noise.



John L. Rice served as an Electronic Technician in the U.S. Navy from 1976 to 1982. He then spent five years as a Contractor in the Naval Calibration Laboratory, Rota, Spain, followed by three years as an Electronic Technician at the Naval Air Test Center, Patuxent River, MD. In 1990, he joined the Noise Project in the Electromagnetic Fields Division of the National Institute of Standards and Technology (NIST), Boulder, CO. Since early 1998, he has been an electronic systems analyst with the National Weather Service, Marquette, MI.